Rachael Muschalek
Biomedical Engineering,
Texas A&M University,
College Station, TX 77843
e-mail: rmuschalek2015@gmail.com

Landon Nash
Biomedical Engineering,
Texas A&M University,
College Station, TX 77843;
Shape Memory Medical, Inc.,
Santa Clara, CA 95054
e-mail: nashlandon@gmail.com

Ryan Jones
Biomedical Engineering,
Texas A&M University,
College Station, TX 77843
e-mail: jonesrya@tamu.edu

Sayyeda M. Hasan
Biomedical Engineering,
Texas A&M University,
College Station, TX 77843;
Shape Memory Medical, Inc.,
Santa Clara, CA 95054
e-mail: marziyahasan@gmail.com

Brandis K. Keller
Biomedical Engineering,
Texas A&M University,
College Station, TX 77843
e-mail: bkeller@tamu.edu

Mary Beth B. Monroe
Biomedical Engineering,
Texas A&M University,
College Station, TX 77843
e-mail: mbbmonroe@tamu.edu

Duncan J. Maitland
Biomedical Engineering,
Texas A&M University,
College Station, TX 77843;
Shape Memory Medical, Inc.,
Santa Clara, CA 95054
e-mail: djmaitland@tamu.edu

Effects of Sterilization on Shape Memory Polyurethane Embolic Foam Devices

Polyurethane shape memory polymer (SMP) foams have been developed for various embolic medical devices due to their unique properties in minimally invasive biomedical applications. These polyurethane materials can be stored in a secondary shape, from which they can recover their primary shape after exposure to an external stimulus, such as heat and water exposure. Tailored actuation temperatures of SMPs provide benefits for minimally invasive biomedical applications, but incur significant challenges for SMP-based medical device sterilization. Most sterilization methods require high temperatures or high humidity to effectively reduce the bioburden of the device, but the environment must be tightly controlled after device fabrication. Here, two probable sterilization methods (nontraditional ethylene oxide (ntEtO) gas sterilization and electron beam irradiation) are investigated for SMP medical devices. Thermal characterization of the sterilized foams indicated that ntEtO gas sterilization significantly decreased the glass transition temperature. Further material characterization was undertaken on the electron beam (ebeam) sterilized samples, which indicated minimal changes to the thermomechanical integrity of the bulk foam and to the device functionality. [DOI: 10.1115/1.4037052]

1 Introduction

Recent advances in material science have increased the use of polymers for biomedical applications [1]. Stimuli responsive polymers, such as shape memeory polymers (SMPs), have shown promise in polymer-based medical devices for multiple applications, including thrombus removal devices, cardiac valve repair devices, and various embolic devices [2–6]. SMPs are a class of smart material that are capable of being deformed and stored in a stable secondary shape and recovering to a primary form when exposed to a stimulus, such as heat [2,3,7,8]. This shape memory property allows for noninvasive or minimally invasive implantable medical devices, as SMPs can be stored in a compressed form during delivery, after which they expand to their primary shape upon heating to body temperature [2,7–10].

Polyurethane SMP foams have been previously synthesized with excellent embolic and healing responses [11,12]. These polyurethane foams show promise for treatment of a variety of vascular malformations or traumatic injuries [2,13]. Preliminary efforts have focused on functionality and fabrication of a device [9,10], but other hurdles must be overcome to realize the clinical potential of these SMP-based devices; such as a validated sterilization method to gain regulatory approval [14–17].

The proposed thermoset polyurethanes have excellent shape memory capacity due to their extensive crosslinking [18], but chain–chain hydrogen bonding influences the temperature at which these polymers actuate. Disruption of this hydrogen-bonding network can occur *via* plasticizers, the most common of which is water [7]. In the case of stimuli-responsive polymers, plasticization can drastically reduce the actuation temperature at

Manuscript received August 3, 2016; final manuscript received May 9, 2017; published online June 28, 2017. Assoc. Editor: Michael Eggen.

which shape recovery occurs [7]. The shape memory aspect of these foams is dependent upon a combination of moisture plasticization and thermal actuation from heating to body temperature [7,9,10]. Premature actuation could lead to the polymer system expanding within the delivery catheter and subsequent failure of the medical device [7,9,10]. Thus, a major hurdle for medical device approval is sterilization of this heat and moisture sensitive polymer system while minimizing the chance of premature actuation.

Many options are available for sterilization of implantable medical devices [15,19–22]. This research looks into two potential sterilization methods for the polyurethane SMP embolic foams: nontraditional ethylene oxide (ntEtO) gas sterilization [10] and electron beam irradiation (ebeam). Traditional ethylene oxide (a higher heat and humidity process as compared to ntEtO) and gamma radiation were eliminated from this study due to an unfavorable sterilization environment and discouraging pilot data, respectively. Plasma sterilization was also considered for sterilization of polyurethane SMP foams due to its low temperature profiles; however, the use of photons and radicals could oxidize the foam surface [22,23]. We hypothesized that these surface chemistry changes would alter the overall hydrophobicity and therefore significantly decrease the working time (amount of time that a clinician has for delivery) of the final device. Thus, we did not include plasma sterilization in these studies. ntEtO gas sterilization requires gaseous diffusion into the packaging in order for the gas to interact with the microbes on the device [20]. For safety reasons, porous materials are required to aerate for at least 12 h after ntEtO sterilization [20]. Electron beam radiation uses an electron linear accelerator to sterilize the devices and has a much quicker turnaround time [24].

Each sterilization system utilizes specialized packaging to allow penetration of the gas and/or energy to ensure that sterility is maintained during storage. Nitrogen purged, vacuum-sealed foil pouches are used to limit oxygen and moisture diffusion in the packaging that could lead to polymer oxidation during irradiation. Packaging with gas permeable films segments, such as foil header pouches (Beacon Converters, Saddle Brook, NJ), is necessary for effective ntEtO sterilization. These gas permeable segments, or headers, enable EtO gas and moisture diffusion into the pouch for effective sterilization and subsequent EtO off-gassing. Although moisture diffusion is required for ntEtO, the previous work suggested that the off-gassing in this process would limit plasticization of SMP foams to provide an acceptable sterilization option [25]. Moisture is important for effectively killing desiccated bacterial spores during sterilization, and residual EtO must be effectively removed prior to device implantation. After sterilization, these gas permeable segments can be sealed and removed to prevent further moisture diffusion and prolong shelf life for moisture sensitive materials.

Sterilized devices were characterized using tensile testing, differential scanning calorimetry (DSC), crimp diameter characterization, unconstrained cylindrical expansion, and Fourier transform infrared (FTIR) spectroscopy. This was done in an effort to assess the effects of sterilization on device performance and determine a feasible sterilization method for these SMP foams.

2 Materials and Methods

2.1 Materials. N,N,N′,N′-tetrakis(2-hydroxypropyl)ethylenediamine (HPED, 99%; Sigma-Aldrich, Inc., St. Louis, MO), triethanolamine (TEA, 98%; Sigma-Aldrich Inc., St. Louis, MO), trimethyl-1,6-hexamethylene diisocyanate, 2,2,4- and 2,4,4-mixture (TMHDI; TCI America, Inc., Portland, OR), hexamethylene diisocyanate (HDI; TCI America, Inc., Portland, OR), DC 198 (Air Products and Chemicals, Inc., Allentown, PA), DC 5943 (Air Products and Chemicals, Inc., Allentown, PA), T-131 (Air Products and Chemicals, Inc., Allentown, PA), BL-22 (Air Products and Chemicals Inc., Allentown, PA), Enovate 245fa Blowing Agent (Honeywell International Inc., Houston, TX), 2-propanol 99% (IPA) (VWR, Radnor, PA), and de-ionized (DI) water (E-Pure water system, Barnstead International, Dubuque, IA) were used as received.

2.2 Foam Synthesis. Three different SMP foam formulations, shown in Table 1, were synthesized using the three-step protocol previously described by Hasan et al. [26,27]. Briefly, isocyanate (NCO) prepolymers were synthesized using appropriate molar ratios of HPED, TEA, TMHDI, and HDI, with a 35 wt % hydroxyl (OH) composition. An OH mixture was prepared with the remaining molar equivalents of HPED and TEA, along with catalysts, surfactants, and DI water. During foam blowing, a physical blowing agent, Enovate, was mixed with the isocyanate prepolymer and the OH mixture using a speedmixer (FlakTek, Inc., Hauschild, Germany). The resulting foams were cured in a vacuum oven (Cascade Tek, Hillsboro, OR) at 90 °C for 20 min. The SMP foams were cooled to room temperature (21 ± 1 °C) followed by a 24-h cold cure (21 ± 1 °C) before further processing.

2.3 Cleaning. Foams were cut using a resistively heated wire cutter (Proxxon Thermocut, Prox-Tech, Inc., Hickory, NC) into 2 mm thick slices. The foam slices were shaped using a calibrated and certified ASTM Die D-638 Type IV dog bone punch (Pioneer-Dietecs Corporation, Weymouth, MA). The dog bone samples were utilized for mechanical testing, DSC, and FTIR. Additional cylindrical samples were cut using biopsy punches (0.039, 0.315, or 0.236 in, according to the device type that the formulation is utilized in), as described in Table 1. Cylindrical samples were used in crimp diameter characterization and unconstrained expansion testing. Samples were submerged in 1000 mL jars filled with IPA and sonicated for 2 × 15 min, refreshing the IPA between cycles. Reverse osmosis (RO) water was used as a final wash for 15 min under sonication. Samples were removed, allowed to air dry, and then dried at 100 °C under vacuum for 12 h. Cylindrical samples were threaded axially around a 0.008 in nickel-titanium (nitinol) backbone wire and radially compressed to the smallest possible diameter using a heated SC250 Stent Crimper (Machine Solutions, Inc., Flagstaff, AZ).

2.4 Packaging. Due to variability in the gas blowing process, control foams were taken from each foam batch prior to packaging for sterilization. Samples designated for sterilization were packaged in various sizes of foil header pouches (Tyvek Foil Pouches, Beacon Converters, Saddle Brook, NJ) using an AVN packaging system (AmeriVacS, San Diego, CA). Pouches were purged with nitrogen prior to vacuum sealing with heat. Included in all packages were a temperature indicator (S-6710 Telatemp Heat Indicator, Uline, Pleasant Prairie, WI) and a humidity indicator (S-8028 10–60% Humidity Indicator, Uline, Pleasant Prairie, WI). Dog bone SMP samples were secured inside the package using adhesive and wire. Cylindrical samples were attached with adhesive on each end. Samples designated for ntEtO sterilization were sealed above a header that allowed gaseous exchange during sterilization and degassing. The headers were then sealed and removed to limit further moisture diffusion. Samples designated for radiation-based sterilization were completely vacuum-sealed within the foil portion of the pouch to prevent ambient oxygen from entering the pouch.

Table 1 Monomer ratios used in foam synthesis.

Formulation name	Isocyanate (NCO)	HPED (molar eq.)	TEA (molar eq.)	Cylindrical diameter (in)
100TMH60	TMHDI	60	40	0.039
100HDIH40	HDI	40	60	0.315
100HDIH60	HDI	60	40	0.236

2.5 Sterilization. The ntEtO samples were sterilized with 10.5 g ± 5% of EtO gas into bags of dimension 22 in × 36 in with relative humidity of ≥ 30% at 20 °C injected over 4 h and held for at least 12 h. A biological indicator strip was placed inside the chamber by Anderson Scientific to ensure sterility of the ntEtO samples. Ebeam radiation samples received 40 ± 2.62 kGy (approximately 25 kGy+safety factor of 1.6, according to AAMI/ISO 11137) at the National Center for Electron Beam Research (College Station, TX) using a vertically mounted 10 MeV, 18 kW commercial scale linear accelerator at a dose rate of approximately 3000 Gy s^{-1} on a cold chain set to 5 °C. Alanine films (Kodak, Rochester, NY) were placed below samples to measure actual absorbed radiation dose using a Bruker E-scan spectrometer (Bruker, Billerica, MA). The 1.6× safety factor is utilized in sterilization verification and takes into account the chance that a sample may undergo a second run if the first run fails, resulting in exposure to a total of ∼40 kGy of radiation. A second series of ebeam testing was undertaken at 25 ± 1.88 kGy to characterize the effects of a standard sterilization procedure [17].

2.6 Characterization

2.6.1 Differential Scanning Calorimetry (DSC). Foam samples (2–6 mg) were used for glass transition temperature (T_g) analysis by using a Q-200 dynamic scanning calorimeter (DSC) (TA Instruments, Inc., New Castle, DE) to obtain wet and dry thermograms for the foams. Dry samples were stored in a desiccated container and hermetically sealed into aluminum pans. The first cycle consisted of decreasing the temperature to −40 °C at 10 °C·min^{-1} and holding it isothermally for 2 min. The temperature was then increased to 120 °C at 10 °C·min^{-1} and held isothermally for 2 min. In the second cycle, the temperature was reduced to −40 °C at 10 °C·min^{-1}, held isothermally for 2 min, and raised to 120 °C at 10 °C·min^{-1}. T_g was recorded from the second cycle based on the inflection point of the thermal transition curve using TA instruments software. The aluminum tins were vented during this process. Each dry composition was measured at least three times for reproducibility.

Wet samples were prepared by allowing small foam samples to plasticize in 50 °C RO water for at least 10 min. Water was then pressed out using a mechanical press, and samples were tested on a cycle that decreased the temperature to −40 °C at 10 °C·min^{-1} and holding it isothermally for 2 min. The temperature was then increased to 80 °C at 10 °C·min^{-1}. T_g was recorded from the heating cycle as the inflection point on the thermal transition curve. Each wet composition was measured at least three times for reproducibility.

2.6.2 Mechanical Testing. Each end of the dog bone foam samples was attached to mechanical testing wooden stubs using clear epoxy adhesive and allowed to dry overnight under vacuum. Samples were then strained to failure using an Insight 30 material tester (Materials Testing Solutions, MTS Systems Corporation, Eden Prairie, MN) according to ASTM D638-14 [28]. Stress versus strain curves were analyzed for ultimate tensile stress (UTS) and % strain at break. Each composition was tested at least six times for reproducibility.

2.6.3 Crimp Diameter. Foam cylinders (1–8 mm in diameter) were crimped around a nitinol backbone wire. Diameters for each foam cylinder were chosen according to clinical applicability and can be seen in Table 1. Samples were placed inside the heated chamber of a stent crimper (100 °C) (Machine Solutions, Inc., Flagstaff, AZ) and allowed to equilibrate for 10 min. Crimpers were closed and cooled using room temperature air. Images were taken on a Jenoptik Microscope Camera (Jenoptik, Jena, Germany) 24 h after crimping to generate a baseline of device diameter prior to sterilization. IMAGEJ (NIH, Bethesda, MD) processing software was used to quantify the device diameters prior to sterilization. Upon receipt of devices after sterilization, images were taken again, and device diameter was remeasured. Any device expansion due to plasticization or process-related heating was

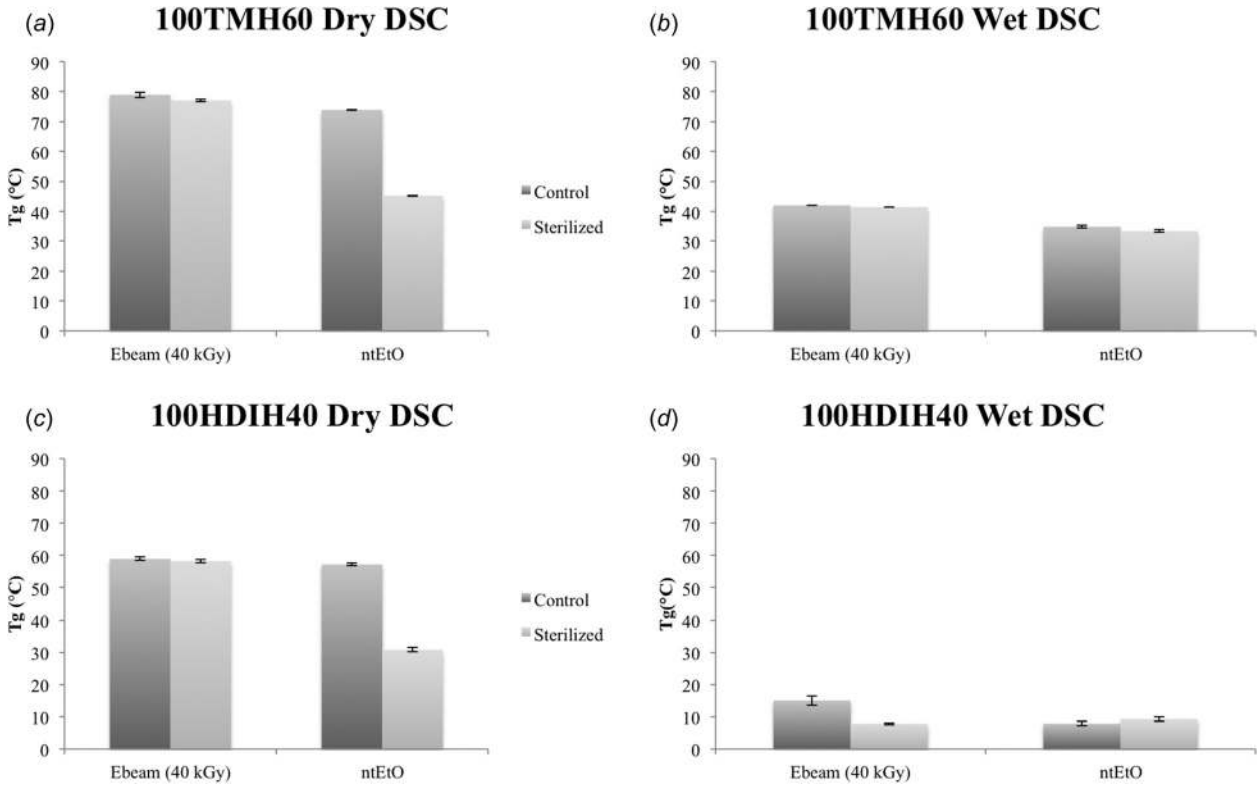

Fig. 1 T_g measurements for the two foam compositions (*a* and *b*: 100TMH60; *c* and *d*: 100HDID40) in wet (*a* and *c*) and dry (*b* and *d*) conditions. *N* = 3, mean ± standard deviation displayed.

noted. Each composition was measured at least three times for reproducibility.

2.6.4 Unconstrained Expansions. Unconstrained expansion of cylindrical samples was assessed in a hot water bath to obtain actuation profiles. Devices were placed on a fixture and submerged in a 37 °C hot water bath. Images were taken with a digital camera (PowerShot SX230 HS, Canon, Inc., Tokyo, Japan) every 30 s for 15 min and analyzed with IMAGEJ image processing software (National Institutes of Health, open source) to quantify device diameter over time. Each composition was measured three times for reproducibility.

2.6.5 Fourier Transform Infrared (FTIR) Spectroscopy. Foam samples were cut to 2–3 mm thick, and the FTIR spectra were collected using Bruker ALPHA Infrared Spectrometer (Bruker, Billerica, MA). Thirty-two background scans of the empty chamber were taken followed by 64 sample scans of the various foam compositions. FTIR spectra were collected in absorption mode at a resolution of 4 cm^{-1}. OPUS software (Bruker, Billerica, MA) was utilized to subtract the background scans from the spectra, to conduct a baseline correction for IR beam scattering and to normalize multiple spectra to one another. Each composition was measured three times for reproducibility and one spectrum was chosen to display.

2.6.6 Statistical Analysis. All the data were expressed as the mean ± standard derivation of the mean. Statistical analysis was performed using the unpaired Student's *t*-test, and statistical significance was accepted at $p < 0.05$.

3 Results

For the majority of the testing, the most and least hydrophilic foam compositions (100HDIH40 and 100TMH60, respectively) were chosen for characterization. Further classification of electron beam radiation was also carried out on 100HDIH60 foams (mid-range hydrophilicity) with multiple radiation doses (25 kGy and 40 kGy).

3.1 Differential Scanning Calorimetry (DSC). The results of the DSC analysis are seen in Figs. 1(*a*)–1(*d*). Thermal analysis shows the largest change in T_g for ntEtO-sterilized dry samples (39% change between control and sterilized sample). Ebeam sterilization produced consistent thermal behavior for all foam compositions and thermal tests. The thermograms of wet DSC measurements for 100HDIH40 foams (Fig. 1(*d*)) were difficult to read due to the proximity of the T_g to the recrystallization peak of water at 0 °C [29]. Thus, these results were not considered to be reliable indications of the effects of sterilization.

3.2 Mechanical Testing. Figures 2 and 3 give the ultimate tensile strength (UTS) and strain at break, respectively, for each foam composition before and after sterilization. The large standard deviations arise from the intrinsic properties of the gas blown foam due to the inhomogeneous pore size and shape. No statistically significant differences in UTS or strain at break were seen following the two sterilization methods for each composition ($p < 0.05$). The batch variability in the gas blowing process becomes evident here, as the two 100TMH60 control foams have

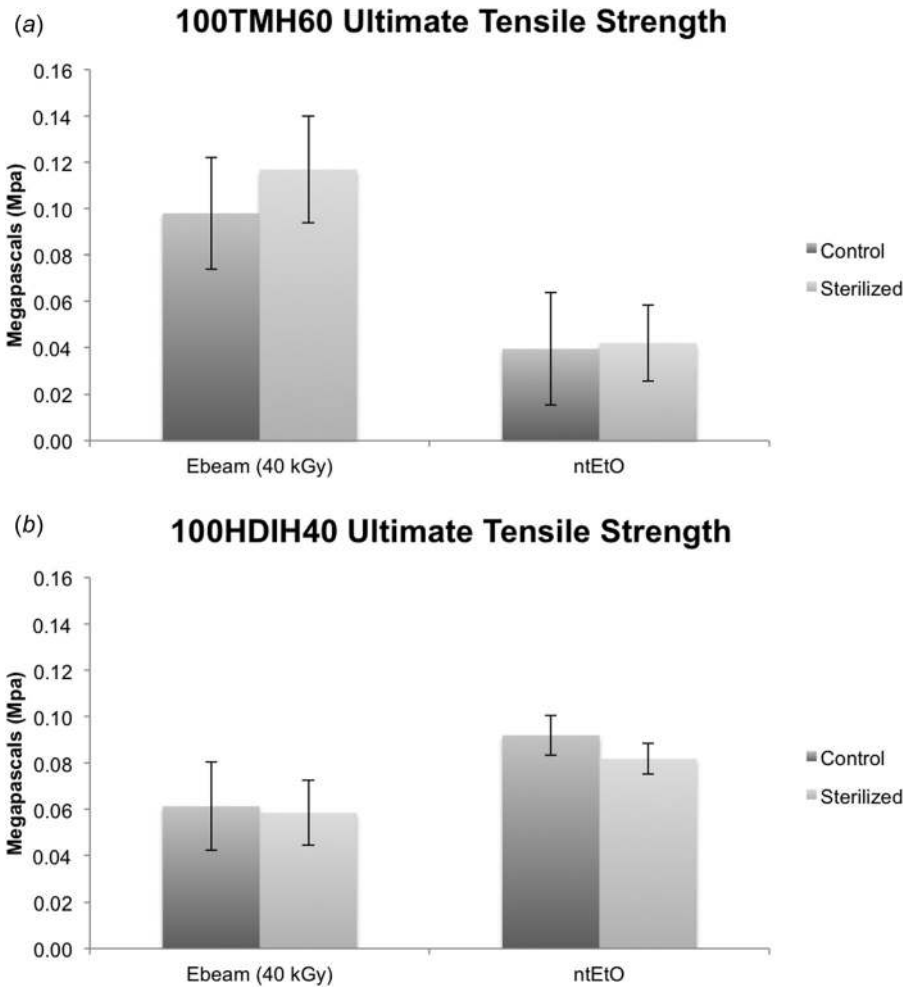

Fig. 2 UTS of (*a*) 100TMH60 and (*b*) 100HDIH40 foams. $N = 6$, mean ± standard deviation displayed.

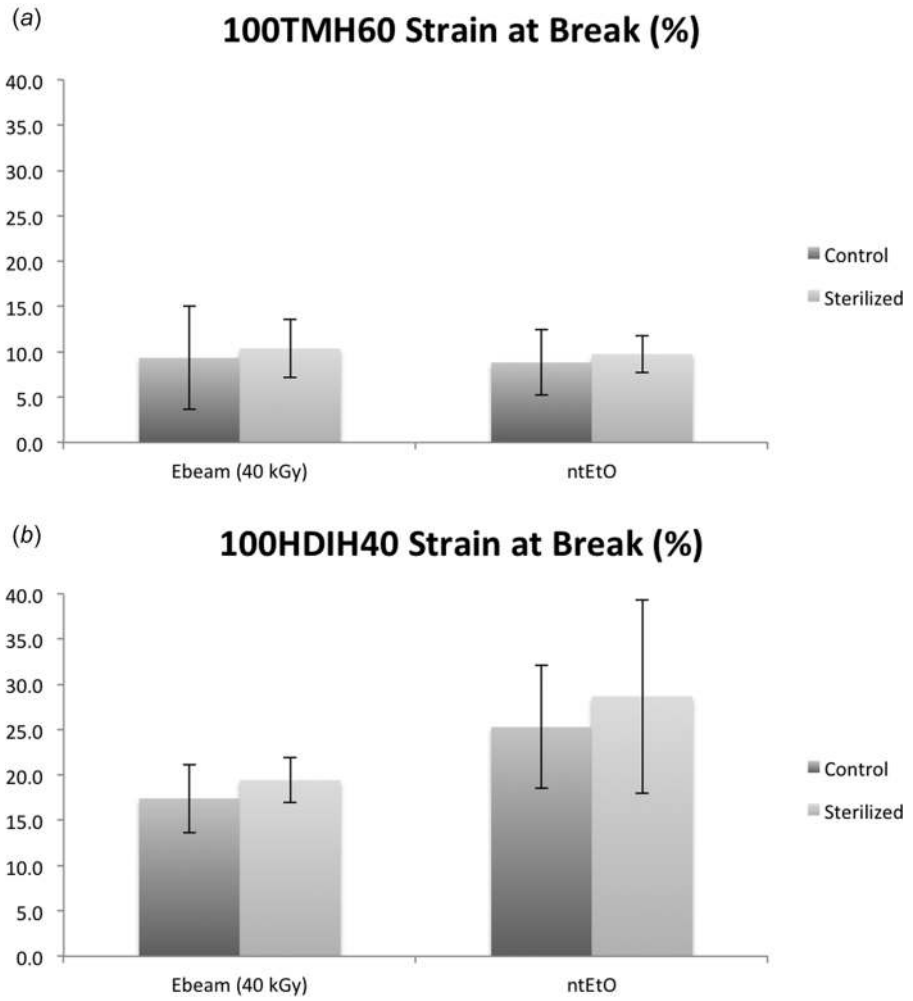

Fig. 3 Strain at break of (*a*) 100TMH60 and (*b*) 100HDIH40 foams. *N* = 6, mean ± standard deviation displayed.

different ultimate tensile strengths. However, the purpose of this study is to evaluate the effects of sterilization. Thus, we ensured that sterilized foams were compared only to controls from the same foam batch.

Table 2 Cylindrical expansion of 100TMH60 foams following sterilization. *N* = 7, mean ± standard deviation displayed.

Sterilization process	Initial diameter (in)	Final diameter (in)	Change in diameter (in)	Change in diameter (%)
Control	0.0147 ± 0.0008	0.0154 ± 0.0007	0.0007	4.76
ntEtO	0.0145 ± 0.0006	0.0163 ± 0.0011	0.0018	12.41
Ebeam (25 kGy)	0.0145 ± 0.0007	0.0158 ± 0.0004	0.0013	8.97

Table 3 Cylindrical expansion of 100HDIH40 foams following sterilization. *N* = 3, mean ± standard deviation displayed.

Sterilization process	Initial diameter (in)	Final diameter (in)	Change in diameter (in)	Change in diameter (%)
Control	0.043 ± 0.007	0.051 ± 0.004	0.008	18.60
ntEtO	0.050 ± 0.002	N/A	N/A	N/A
Ebeam (25 kGy)	0.041 ± 0.005	0.041 ± 0.001	0.000	0.00

3.3 Crimp Diameter. The results of the crimp diameter tests can be seen in Tables 2 and 3. Some relaxation of the crimp is expected to occur, as seen in the control samples, which were left in a dry box for 1 week [30]. It should be noted that "N/A" for ntEtO in the 100HDIH40 samples indicates expansion beyond the constraints of the packaging that prevented imaging of final devices. Ebeam-sterilized cylinders expanded the least, indicating minimal process plasticization; thus, ebeam sterilization was

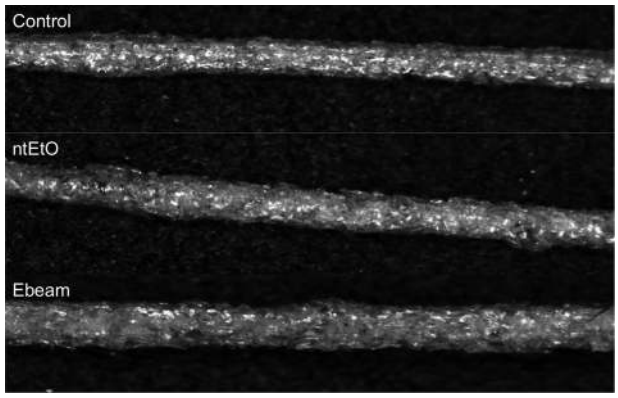

Fig. 4 Cylindrically crimped 1 mm 100TMH60 foam after sterilization

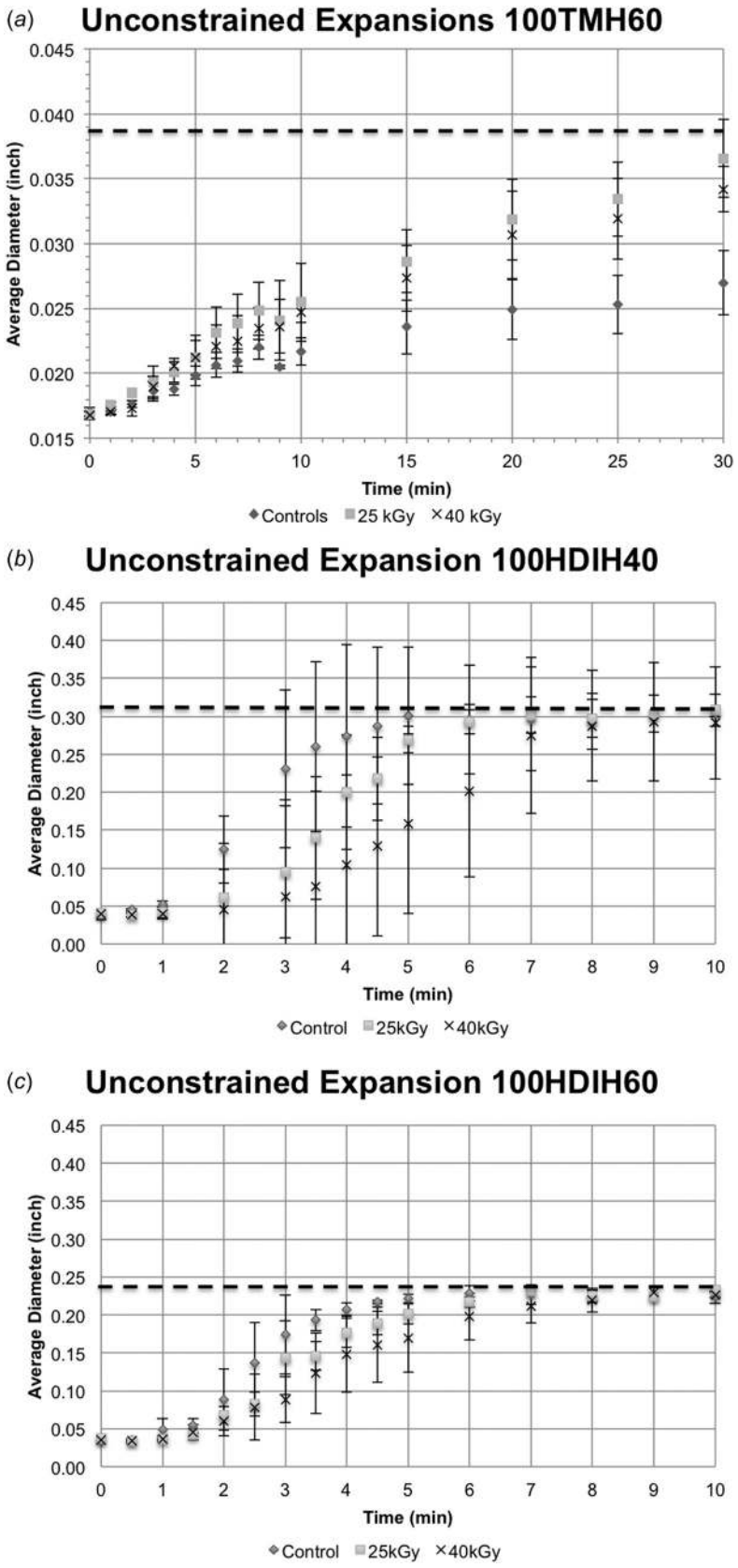

Fig. 5 Unconstrained expansion over time of exposure to 37 °C water for ebeam sterilized (*a*) 100TMH60, (*b*) 100HDIH40, and (*c*) 100HDIH60 foams. $N = 3$, mean ± standard deviation displayed. Dotted line indicates initial cut diameter dimensions.

chosen for further material classification following application of lower radiation dosage (Fig. 4).

3.4 Unconstrained Expansion. To fully characterize ebeam sterilization, 100HDIH60 was added to the two previously characterized foams (100TMH60 and 100HDIH40). All three compositions were exposed to two separate radiation doses (25 kGy and 40 kGy) and utilized in further material characterization. Unconstrained cylindrical expansion of ebeam sterilized samples can be seen in Fig. 5. Both of the HDI compositions (100HDIH40 and 100HDIH60) were fully expanded to their original diameters (8 mm for 100HDIH40 and 6 mm for 100HDIH60) within 10 min, while the TMDHI composition (100TMH60) did not achieve full recovery (1 mm) after 30 min of testing. The 100TMH60 foam exhibited faster expansions with any exposure to radiation as compared to control (Fig. 5(*a*)), while the 100HDIH40 and

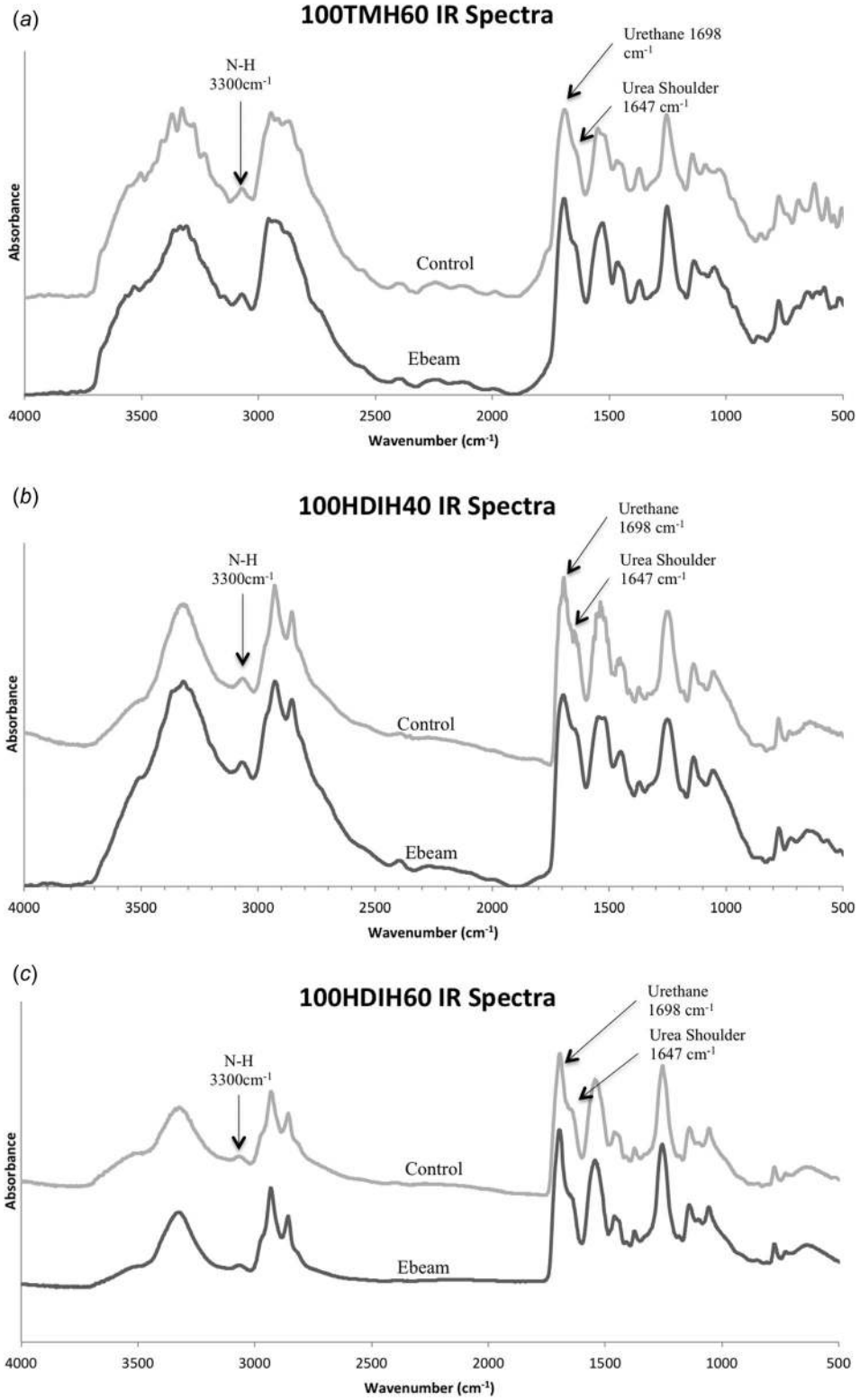

Fig. 6 FTIR spectra of (*a*) 100TMH60, (*b*) 100HDIH40, and (*c*) 100HDIH60 before and after ebeam sterilization at 40 kGy

100HDIH60 both exhibited slower expansion with increasing radiation dose (Figs. 5(*b*) and 5(*c*)). This difference is not fully understood and will be the focus of future studies.

3.5 Fourier Transform Infrared (FTIR) Spectroscopy. FTIR was used to detect any molecular differences that may have arisen during ebeam radiation on the three foam compositions. Selected FTIR spectral regions for the foam compositions can be seen in Fig. 6. No noticeable differences were detected between the control compositions and the ebeam sterilized compositions, indicating that radiation did not induce a significant molecular change in the foam samples. A potential expected change in spectra included oxidative degradation of the tertiary amine [21] which could be seen by an increase in the absorbance at 3400, indicating an increased –NH stretch poststerilization [31].

4 Discussion

The goal of this study was to identify and characterize a sterilization method that would not disrupt the functionality of a SMP foam-based medical device. In addition to the tested methods, traditional ethylene oxide (EtO) is another common sterilization option for medical devices [19]. Due to the failure of the ntEtO-tested foam cylinders as noted by the large decrease in T_g, traditional EtO, which is a higher-heat, higher-humidity process, was removed as a potential sterilization method. Gamma radiation is also a common method for radiation sterilization but was not further investigated in this manuscript due to the higher potential for oxidative degradation as compared to ebeam [21,32].

Ebeam radiation showed the most promise for SMP-based medical devices. Ebeam sterilization resulted in consistent thermal, mechanical, and shape memory properties between control foams and sterilized foams. ntEtO-sterilized foams appeared to have been moisture-plasticized during sterilization, as evidenced by a reduced T_g and increased diameter that prevented expansion characterization. This result is likely due to the relatively long exposure to the humidity (30%) in ntEtO in the moisture-permeable packaging. Ebeam-sterilized devices retained similar expansion profiles to controls with varied dosages and foam compositions. Volume expansion and working time are two of the most important functional considerations for SMP foam devices, as they define how effective a foam will be at shape-filling a defect site and how long a clinician has to deliver the device through the catheter before it expands and restricts delivery of the device, respectively. Maintenance of device function following sterilization is essential in successfully obtaining FDA clearance. Further characterization of electron beam-sterilized foams indicated that no significant molecular changes occur during sterilization. Oxidation is a large concern for SMP foams, as it could alter long-term stability and performance. Thus, a reduced potential of oxidation following ebeam sterilization is highly promising for SMP foam-based medical device development. Future studies include sterilization validation of ebeam-exposed samples to evaluate bioburden, dose verification, bacteriostasis/fungistasis, and growth promotion under varied cycle conditions.

5 Conclusions

In summary, SMP foam properties were tested before and after two common sterilization methods. It was found that ebeam sterilized SMPs were the most functional after sterilization as compared to ntEtO sterilization. The results from this study are critical to the clinical realization of SMP foam-based devices by identifying a reliable sterilization method for future preclinical safety and efficacy studies.

Acknowledgment

This work was supported by the Texas A&M University Graduate Merit Fellowship.

Funding Data

- National Institute of Neurological Disorders and Stroke (U01-NS089692)

References

[1] Ratner, B. D., Hoffman, A. S., Schoen, F. J., and Lemons, J. E., 2004, *Biomaterials Science: An Introduction To Materials in Medicine*, Academic Press, Cambridge, MA.

[2] Small, W., IV, Singhal, P., Wilson, T. S., and Maitland, D. J., 2010, "Biomedical Applications of Thermally Activated Shape Memory Polymers," J. Mater. Chem., **20**(17), pp. 3356–3366.

[3] Baer, G., Wilson, T., Matthews, D., and Maitland, D., 2007, "Shape-Memory Behavior of Thermally Stimulated Polyurethane for Medical Applications," J. Appl. Polym. Sci., **103**(6), pp. 3882–3892.

[4] Lendlein, A., and Kelch, S., 2002, "Shape-Memory Polymers," Angew. Chem. Int. Ed., **41**(12), pp. 2034–2057.

[5] Maitland, D. J., Small, W., Ortega, J. M., Buckley, P. R., Rodriguez, J., Hartman, J., and Wilson, T. S., 2007, "Prototype Laser-Activated Shape Memory Polymer Foam Device for Embolic Treatment of Aneurysms," J. Biomed. Opt., **12**(3), p. 030504.

[6] Boyle, A., Weems, A., Hasan, S., Nash, L., Monroe, M., and Maitland, D., 2016, "Solvent Stimulated Actuation of Polyurethane-Based Shape Memory Polymer Foams Using Dimethyl Sulfoxide and Ethanol," Smart Mater. Struct., **25**(7), p. 075014.

[7] Singhal, P., Boyle, A., Brooks, M. L., Infanger, S., Letts, S., Small, W., Maitland, D. J., and Wilson, T. S., 2013, "Controlling the Actuation Rate of Low-Density Shape-Memory Polymer Foams in Water," Macromol. Chem. Phys., **214**(11), pp. 1204–1214.

[8] Singhal, P., Rodriguez, J. N., Small, W., Eagleston, S., Van de Water, J., Maitland, D. J., and Wilson, T. S., 2012, "Ultra Low Density and Highly Crosslinked Biocompatible Shape Memory Polyurethane Foams," J. Polym. Sci. Part B: Polym. Phys., **50**(10), pp. 724–737.

[9] Hwang, W., Singhal, P., Miller, M. W., and Maitland, D. J., 2013, "In Vitro Study of Transcatheter Delivery of a Shape Memory Polymer Foam Embolic Device for Treating Cerebral Aneurysms," ASME J. Med. Devices, **7**(2), p. 020932.

[10] Boyle, A. J., Landsman, T. L., Wierzbicki, M. A., Nash, L. D., Hwang, W., Miller, M. W., Tuzun, E., Hasan, S. M., and Maitland, D. J., 2016, "In Vitro and In Vivo Evaluation of a Shape Memory Polymer Foam-Over-Wire Embolization Device Delivered in Saccular Aneurysm Models," J. Biomed. Mater. Res. Part B: Appl. Biomater., **104**(7), pp. 1407–1415.

[11] Rodriguez, J. N., Clubb, F. J., Wilson, T. S., Miller, M. W., Fossum, T. W., Hartman, J., Tuzun, E., Singhal, P., and Maitland, D. J., 2014, "In Vivo Response to an Implanted Shape Memory Polyurethane Foam in a Porcine Aneurysm Model," J. Biomed. Mater. Res. Part A, **102**(5), pp. 1231–1242.

[12] Horn, J., Hwang, W., Jessen, S. L., Keller, B. K., Miller, M. W., Tuzun, E., Hartman, J., Clubb, F. J., and Maitland, D. J., 2016, "Comparison of Shape Memory Polymer Foam Versus Bare Metal Coil Treatments in an In Vivo Porcine Sidewall Aneurysm Model," J. Biomed. Mater. Res. Part B: Appl. Biomater., epub.

[13] Small, W., IV, Wilson, T. S., Benett, W. J., Loge, J. M., and Maitland, D. J., 2005, "Laser-Activated Shape Memory Polymer Intravascular Thrombectomy Device," Opt. Express, **13**(20), pp. 8204–8213.

[14] Kotzar, G., Freas, M., Abel, P., Fleischman, A., Roy, S., Zorman, C., Moran, J. M., and Melzak, J., 2002, "Evaluation of MEMS Materials of Construction for Implantable Medical Devices," Biomaterials, **23**(13), pp. 2737–2750.

[15] Rutala, W. A., Weber, D. J., and the Healthcare Infection Control Practices Advisory Committee (HICPAC), 2008, "Guideline for Disinfection and Sterilization in Healthcare Facilities," Centers for Disease Control, Atlanta, GA.

[16] ISO, 2009, "Biological Evaluation of Medical Devices—Part 1: Evaluation and Testing Within a Risk Management Process," International Organization for Standardization, Geneva, Switzerland, Standard No. ISO 10993-1:2009.

[17] ISO, 2013, "Sterilization of Health Care Products—Radiation—Part 2: Establishing the Sterilization Dose," International Organization for Standardization, Washington, DC, Standard No. ISO 11137-2:2012.

[18] Wilson, T., Bearinger, J., Herberg, J., Marion, J., Wright, W., Evans, C., and Maitland, D., 2007, "Shape Memory Polymers Based on Uniform Aliphatic Urethane Networks," J. Appl. Polym. Sci., **106**(1), pp. 540–551.

[19] Mendes, G. C., Brandao, T. R., and Silva, C. L., 2007, "Ethylene Oxide Sterilization of Medical Devices: A Review," Am. J. Infect. Control, **35**(9), pp. 574–581.

[20] Rutala, W. A., and Weber, D. J., 2015, "ERCP Scopes: What Can We Do to Prevent Infections?," Infect. Control Hosp. Epidemiol., **36**(6), pp. 643–648.

[21] Premnath, V., Harris, W. H., Jasty, M., and Merrill, E. W., 1996, "Gamma Sterilization of UHMWPE Articular Implants: An Analysis of the Oxidation Problem," Biomaterials, **17**(18), pp. 1741–1753.

[22] De Nardo, L., Alberti, R., Cigada, A., Yahia, L. H., Tanzi, M. C., and Farè, S., 2009, "Shape Memory Polymer Foams for Cerebral Aneurysm Reparation: Effects of Plasma Sterilization on Physical Properties and Cytocompatibility," Acta Biomater., **5**(5), pp. 1508–1518.

[23] Lerouge, S., Wertheimer, M. R., and Yahia, L. H., 2001, "Plasma Sterilization: A Review of Parameters, Mechanisms, and Limitations," Plasmas Polym., **6**(3), pp. 175–188.

[24] Allen, J. T., Calhoun, R., Helm, J., Kruger, S., Lee, C., Mendonsa, R., Meyer, S., Pageau, G., Shaffer, H., Whitham, K., Williams, C. B., and Farrell, J. P., 1995, "A Fully Integrated 10 MeV Electron Beam Sterilization System," Radiat. Phys. Chem., **46**(4–6), pp. 457–460.

[25] Ecker, M., Danda, V., Shoffstall, A. J., Mahmood, S. F., Joshi-Imre, A., Frewin, C. L., Ware, T. H., Capadona, J. R., Pancrazio, J. J., and Voit, W. E., 2016, "Sterilization of Thiol-ene/Acrylate Based Shape Memory Polymers for Biomedical Applications," Macromol. Mater. Eng., **302**(2), pp. 1439–2054.
[26] Hasan, S. M., Harman, G., Zhou, F., Raymond, J. E., Gustafson, T. P., Wilson, T. S., and Maitland, D. J., 2016, "Tungsten-Loaded SMP Foam Nanocomposites With Inherent Radiopacity and Tunable Thermos-Mechanical Properties," Polym. Adv. Technol., **27**(2), pp. 195–203.
[27] Hasan, S. M., Thompson, R. S., Emery, H., Nathan, A. L., Weems, A. C., Zhou, F., Wilson, T. S., and Maitland, D. J., 2016, "Modification of Shape Memory Polymer Foams Using Tungsten, Aluminum Oxide, and Silicon Dioxide Nanoparticles," RSC Adv., **6**(2), pp. 918–927.
[28] ASTM, 2014, "Standard Test Method for Tensile Properties of Plastics," ASTM International, West Conshohocken, PA, Standard No. ASTM D638-14.
[29] Ping, Z. H., Nguyen, Q. T., Chen, S. M., Zhou, J. Q., and Ding, Y. D., 2001, "States of Water in Different Hydrophilic Polymers—DSC and FTIR Studies," Polymer, **42**(20), pp. 8461–8467.
[30] Qi, H. J., and Boyce, M. C., 2005, "Stress–Strain Behavior of Thermoplastic Polyurethanes," Mech. Mater., **37**(8), pp. 817–839.
[31] Coates, J., 2000, "Interpretation of Infrared Spectra, a Practical Approach," *Encyclopedia of Analytical Chemistry*, Wiley, Hoboken, NJ.
[32] Silindir, M., and Ozer, A., 2009, "Sterilization Methods and the Comparison of e-Beam Sterilization With Gamma Radiation Sterilization," FABAD J. Pharm. Sci., **34**(34), pp. 43–53.